Open Access

Iraqi Journal of Industrial Research (IJOIR)

Journal homepage: http://ijoir.gov.iq

Preparation and Characterization of Chitosan/Ag_2O NP Biocomposites for Tetracycline Adsorption

Ahmed L. Majeed*, Juman A. Naser

Department of Chemistry, College of Education for Pure Sciences (Ibn Al-Haitham), University of Baghdad, Iraq

Article information

Article history:
Received: August, 07, 2025
Accepted: September, 02, 2025
Available online: December, 14, 2025

Keywords:
Nano composite,
Silver oxide,
Chitosan,
Tetracycline

Corresponding Author:
Ahmed L. Majeed
Ahmed.Labeeb2105p@ihcoedu.uobaghdad.edu.iq

DOI:
https://doi.org/10.53523/ijoirVol12I2ID596

Abstract

The large-scale contamination of water resources by antibiotics, particularly tetracycline (TC), represents a massive threat. In the present study, the synthesis, characterization, and application of chitosan/Ag_2O NP biocomposites as efficient adsorbents for the elimination of TC from aqueous solutions were investigated. Silver oxide nanoparticles (Ag_2O NPs) were synthesized using the co-precipitation method and incorporated into a chitosan matrix to enhance adsorption capacity. The resulting biocomposite was characterized using Fourier-transform infrared spectroscopy (FTIR), X-ray diffraction (XRD), scanning electron microscopy (SEM), energy dispersive X-ray spectroscopy (EDS), and atomic force microscopy (AFM) to evaluate its structural, morphological, and functional properties. Adsorption parameters such as adsorbent mass, contact time, initial concentration, and temperature were systematically studied. The maximum adsorption capacity of 51.422 mg/g was achieved at 303 K after 60 min using 0.08 g of the synthesized composite. Adsorption isotherm data were analyzed using the Freundlich, Temkin, and Langmuir models, with the results showing better agreement with the Temkin and Freundlich models. Furthermore, temperature played a significant role, as the removal efficiency decreased with increasing temperature, confirming the exothermic nature of the adsorption process. Thermodynamic analysis further supported this observation, with negative $\Delta H°$ (–23.75 kJ/mol) indicating an exothermic process, positive $\Delta G°$ values (+4.08 to +5.93 kJ/mol) indicate non-spontaneity under the studied conditions, and negative $\Delta S°$ values (–90 to –92 J/mol.K) reflecting decreased randomness at the solid–liquid interface during adsorption.

1. Introduction

Contaminated water has grown to be an important problem in the world, made worse by various substances including pharmaceutical products, wastes produced by industries, and heavy metals [1]. Antibiotics like TC are particularly alarming owing to their persistence, toxicity, and resistance to conventional degradation approaches [2]. Being a major ingredient in both medical and veterinary practices, TC is discharged into the aquatic environment through wastewater from pharmaceutical industries, hospitals, and agricultural activities [3].

Such pollution endangers aquatic organisms and creates risks to human beings by promoting antibiotic resistance and disturbing ecosystems [4]. Therefore, it is essential to decrease the concentrations of TC in wastewater, making it an urgent focus of current research [2].

Several techniques have been employed for the removal of TC from water, including advanced oxidation processes (AOPs) such as photo catalysis and ozonation, membrane filtration methods like nanofiltration, and biological treatments including activated sludge [5] However, these methods often face challenges such as high operational costs, energy consumption, membrane fouling, and incomplete degradation. In contrast, adsorption has gained growing popularity due to its effectiveness, low cost, simplicity, and ability to remove a wide range of pollutants, including antibiotics, from aqueous solutions [6].

A sustainable water treatment method is using natural materials, especially biopolymers, as adsorbents. One such biopolymer is chitosan which is derived from chitin and it has been lately considered for its superb characteristics such as biocompatibility, biodegradability and functional surfaces. Since chitosan is capable of binding with pollutants via coordination, chelation, and electrostatic interactions, it has the potential for adsorption applications. Nonetheless, attachments comprising enhanced functionality need to be made to address issues such as low mechanical strength and low adsorbent efficiency in some applications as well as low solubility in acidic environments [7, 8].

More recently, it has been reported that composite materials containing chitosan and Nano-hybrids have better physical-chemical stability, better mechanical properties, as well as better adsorption capacity. In particular, Ag_2O NPs were one of the additive materials attracting attention as a result of their elevated antimicrobial activity, expanded external area, and unique electrical characteristics which are beneficial in pollutant removal and degradation. The combination of chitosan and Ag_2O NPs results in the formation of biocomposites which are claimed to counterbalance the disadvantages of both materials. These composites not only are able to adsorb TC efficiently but also demonstrate antimicrobial activity making them suitable candidates for water treatment processes [9].

Chitosan/Ag_2O NP biocomposites are generally fabricated through in-situ synthesis, solution casting, or chemical cross-linking methods which are relatively simple. These methods facilitate the functionality of Ag_2O NPs to be incorporated within the chitosan framework which magnifies the presence of adsorption regions, increases the surface area and enhances stability. The characterization of these composites using FTIR, SEM, AFM, and EDS, among other techniques, elucidated their structural, elemental, and functional properties. This information is crucial for enhancing their efficiency in real water treatment applications [10].

The composite used in this study consists of chitosan and Ag_2O NPs, forming a chitosan/Ag_2O NPs biocomposite, which has been reported to be effective in the removal of TC under various factors, including pH, concentration, and temperature of the pollutants. These outcomes emphasize the adaptability and applicability of these materials for practical use. In addition, the fact that these composites can be reused while consistently achieving high adsorption efficiencies over several cycles makes them a more sustainable option for managing wastewater in the long term. However, closer investigation is required to overcome issues such as the scale of manufacture of the chitosan/Ag NPs composites, environmental concerns regarding silver nanoparticles (Ag NPs), and the economics of mass production [11].

By integrating nanotechnology and biopolymer science in the synthesis of chitosan/Ag_2O NP biocomposites, a multi-dimensional strategy is implemented in the fight against water pollution. With the increasing population and the subsequent need for clean water, the future seems bright for these novel materials in providing solutions that are both efficient and environmentally friendly in treating wastewater. These activities include the preparation and characterization of chitosan/Ag_2O NP biocomposites, which are expected to have high potential for TC adsorption one of the objectives of this study thereby contributing to the development of this emerging field. Therefore, this study aims to synthesize and characterize chitosan/Ag_2O NP biocomposites and evaluate their potential for TC adsorption from aqueous solutions. The study also investigates the effects of adsorbent

mass, initial TC concentration, and contact time on adsorption efficiency, as well as examines the thermodynamic behavior of the adsorption process.

2. Experimental Procedure

2.1. Chemicals

Table (1): Chemical compounds used in this study, with formula, purity, molar mass, and sources.

No.	Chemicals	Formula	Molar mass (g/mol)	Company	Purity or assay (%)
1	Chitosan (HMW)	$(C_6H_{11}NO_6)_n$	161.2	Sigma Aldrich	75
2	Sodium hydroxide	NaOH	40	Sigma Aldrich	98
6	Silver nitrate	$AgNO_3$	169.87	Sigma Aldrich	≥99.0
7	TC	$C_{22}H_{24}N_2O_8$	444.43	Sigma Aldrich	≥99.0

2.2. Preparation of Ag_2O NPs

Ag_2O NPs were prepared in this work using the co-precipitation method [12]. An aqueous silver nitrate solution ($AgNO_3$) with a concentration of 0.006 M and a volume of 750 mL was prepared in a 2000 mL glass beaker. The solution was then heated to 60 °C. Subsequently, 20 mL of 30% sodium hydroxide (NaOH) solution was gradually added while stirring constantly, maintaining the temperature. After the addition, the mixture was continuously stirred for 30 min at the same temperature. The reacted mixture was allowed to cool, and the precipitate was collected. The residual base was removed by washing with hot distilled water. The resulting precipitate was dried in an oven at 100 °C for 90 min. Finally, to obtain nanoparticles, the dried precipitate was calcined in a furnace at 500 °C for 180 min.

2.3. Preparation of Chitosan/Ag_2O NPs Composite

In a 250 mL beaker, 3.8 g of chitosan was dissolved in 80 mLof an aqueous solution containing 1% (v/v) acetic acid and stirred continuously at 50 °C. To prepare the composite material, 0.2 g of Ag_2O NPs was added to 80 mL of the previously prepared chitosan solution while stirring constantly. This procedure yielded a chitosan/Ag_2O NPs composite in the form of a solid powder containing 5% Ag_2O NPs. The resulting mixture was then placed in an oven and heated at 100 °C for 120 min. The final composite was stored in a sealed container and used as a surface adsorbent.

2.4. Preparing the TC Standard Solution

The standard TC solution used in this study was prepared by dissolving 0.25 g of TC in 500 mL of distilled water, resulting in a concentration of 500 ppm.

2.5. Determination of Adsorbent Weight

To determine the optimum adsorbent weight of the chitosan/Ag_2O NPs composite, different masses (0.02, 0.04, 0.06, 0.08, and 0.1 g) were tested while keeping other parameters constant, including temperature, solution concentration, volume, and contact time. Each flask contained 10 mL of a 30 ppm TC solution and was shaken in a water bath. After two hours, the samples were centrifuged, filtered, and analyzed. The optimum adsorbent weight was found to be 0.08 g.

2.6. Determination of Initial Concentration

In five flasks, 10 mL of TC solutions with concentrations of 10, 20, 30, 40, and 50 ppm were prepared, and 0.08 g of the chitosan/Ag_2O NPs composite was added to each flask. The flasks were placed in a temperature controlled water bath at 303 K and shaken until equilibrium was reached after 60 min subsequently, 10 mL from each flask was withdrawn, centrifuged for 5 min at 5000 rpm, and filtered. The absorbance of the supernatant was measured using a UV–Vis spectrophotometer, and the TC concentration was determined from a calibration curve.

2.7. Determination of Contact Time

To determine the equilibrium time for TC adsorption on chitosan, all other parameters, including temperature, adsorbent weight, solution concentration, and volume, were kept constant. Eight 50 mL beakers, each containing 0.08 g of chitosan and 10 mL of 30 ppm TC solution, were prepared. The beakers were placed in a temperature-controlled water bath and shaken continuously. At 15 min intervals, one beaker was withdrawn, and its 10 mL solution was centrifuged at 5000 rpm for 5 min, filtered, and the absorbance of the supernatant was measured. This procedure was repeated until all eight beakers had been analyzed.

2.8. Determination of the Optimal Temperature for TC Removal Efficiency

TC solutions (10–50 mg/L, 10 mL each) were added to 50 mL flasks containing 0.08 g of the chitosan/Ag_2O NPs composite. Separate sets of flasks were prepared for each temperature (303, 313, and 323 K) and shaken in a water bath for 60 min. After centrifugation, the absorbance of the supernatant was measured at 360 nm. The removal percentage was calculated using the equation (1) [13].

$$R\% = \frac{(C_o - C_e)}{C_o} \times 100 \quad \text{..... (1)}$$

Where C_0 and C_e represent the initial and equilibrium concentrations, respectively.

2.9. Adsorption Isotherms

Ten milliliters of TC aqueous solutions with concentrations of 10, 20, 30, 40, and 50 mg/L were added to 50 mL glass flasks, each containing 0.08 g of the chitosan/Ag_2O NPs composite. The flasks were then immersed in a water bath and shaken for 60 min to reach equilibrium. The experiment was conducted sequentially at three different temperatures: first at 303 K, then at 313 K, and finally at 323 K. After each run, the adsorbent and TC solution were separated by centrifugation. The absorbance of the supernatant was measured at 360 nm, the maximum wavelength of TC, using a UV–Vis spectrophotometer. The amount of TC adsorbed (mg/g) was calculated using the equation (2) [14].

$$q_e = \frac{(C_0 - C_e)V}{m} \quad \text{..... (2)}$$

The formula for calculating adsorption capacity is q_e (mg/g), C_e is equilibrium concentration of TC (mg/L), C_0 is the initial concentration of TC (mg/L), where m is the adsorbent mass (g) and V is the volume of the TC solution (L).

3. Results and Discussion

3.1. Characterization of Chitosan/Ag_2O NPs Composite

3.1.1. Fourier-Transform Infrared Spectroscopy (FTIR)

To characterize the chemical groups in the samples, FTIR spectroscopy was utilized due to its effectiveness. Figure (1) displays the FTIR spectrum of Ag_2O NPs, which contains characteristic peaks corresponding to a series of functional groups. Broad peaks observed between 3222.88 cm^{-1} and 3095.17 cm^{-1} were typical of O–H stretching for adsorbed water or hydroxyl groups. A peak around 2097.89 cm^{-1} indicated the presence of carbonyl (C=O) stretching, possibly from organic residues or surface chemistry. Strong absorption bands between 500 and 600 cm^{-1}, with maxima at 586.89, 530.93, 499.36, and 424.74 cm^{-1}, were characteristic of Ag–O bond vibrations, confirming the presence of Ag_2O NPs. Peaks between 1760 cm^{-1} and 1200 cm^{-1} were attributed to other stretching vibrations of organic and inorganic compounds due to surface functionality or impurities. This analysis confirmed the successful synthesis of Ag_2O NPs [15].

Figure (2) displays the FTIR spectrum of chitosan, while Figure (3) shows the FTIR spectrum of the chitosan/Ag_2O NPs composite, exhibiting characteristic bands of chitosan functional groups and their interactions with Ag_2O NPs, confirming the formation of the composite.

The broad bands observed at 3320 cm^{-1}, 3182 cm^{-1}, and 3030 cm^{-1} were assigned to O–H and N–H stretching vibrations, indicating hydroxyl and amine groups in chitosan. Additionally, shifts in peaks corresponding to

chitosan functionalities, such as amide I and amide II at 1674 cm^{-1} and 1570 cm^{-1}, suggested interactions with Ag_2O NPs. Peaks at 2096 cm^{-1} and 1993 cm^{-1} were attributed to C=O stretching, likely from carboxyl or carbonyl functional groups. The region from 1485 cm^{-1} to 1152 cm^{-1} corresponded to C–N and C–O stretching vibrations, further confirming the presence of chitosan.

The most notable changes were observed in the 600–500 cm^{-1} region, with peaks at 657 cm^{-1}, 589 cm^{-1}, 537 cm^{-1}, and 474 cm^{-1}, assigned to Ag–O bond vibrations, confirming the formation of Ag_2O NPs and their immobilization in the chitosan matrix. This analysis clearly highlighted the differences between pure chitosan and the resulting composite, indicating the successful interaction between chitosan and Ag_2O NPs and the formation of the chitosan/Ag_2O NPs composite [16].

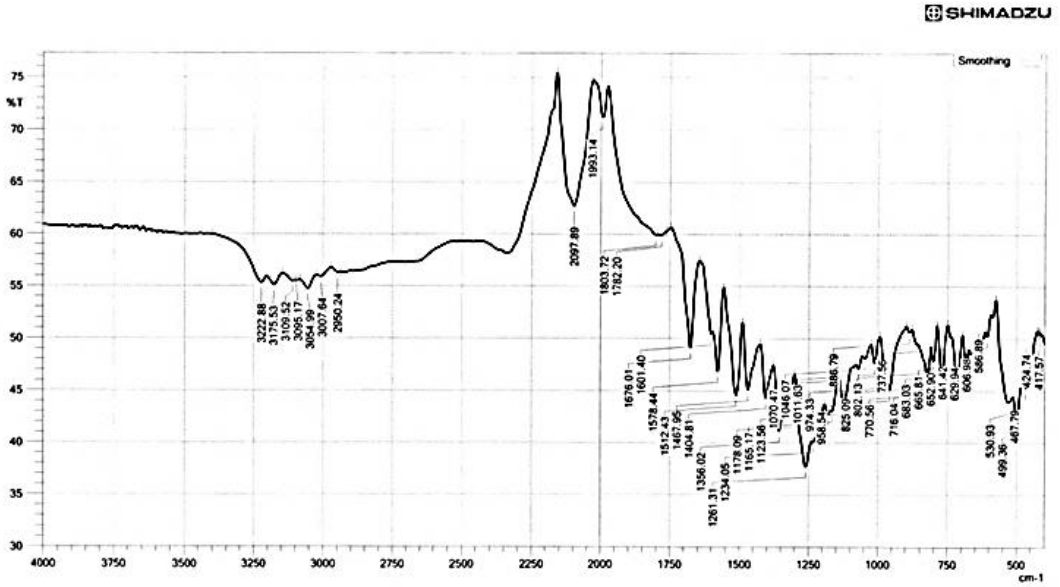

Figure (1): FT-IR spectrum of the synthesized Ag_2O NPs.

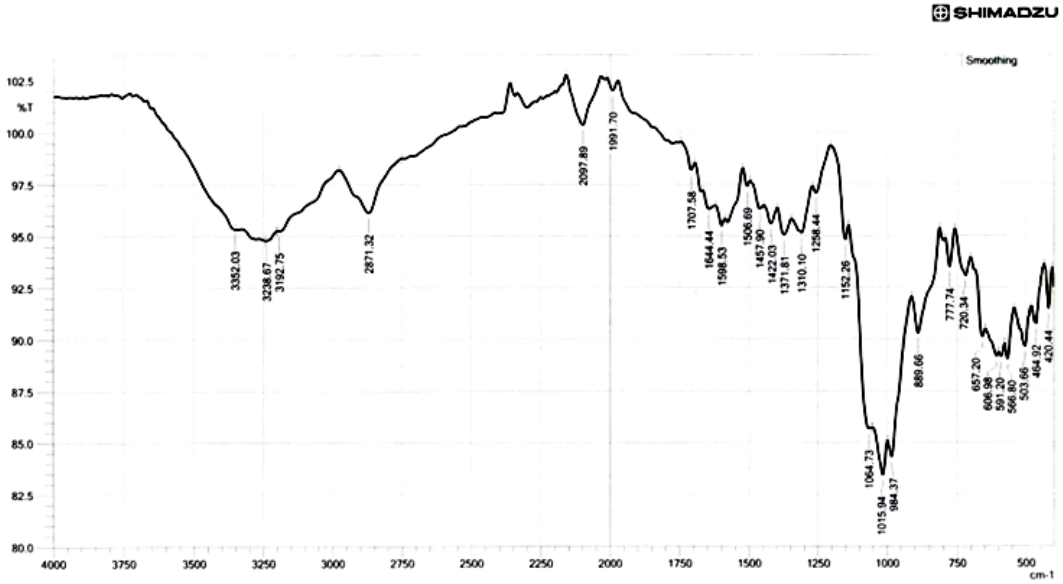

Figure (2): FT-IR spectrum of the chitosan.

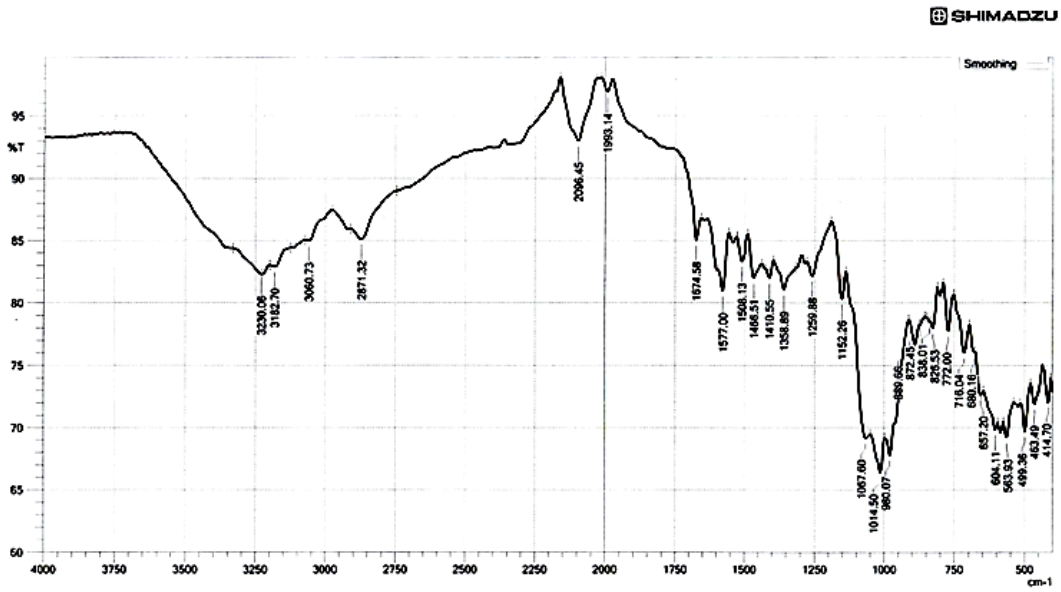

Figure (3): FT-IR spectrum of the synthesized chitosan/Ag_2O NPs composite.

3.1.2. Scanning Electron Microscopy (SEM) for Microstructural Analysis

Figures (4 & 5) show the microscopic images of Ag_2O NPs and the chitosan/Ag_2O NPs composite, respectively, obtained at 500 nm magnification using a scanning electron microscope (SEM). The microscopic images revealed that Ag_2O NPs were spherical in shape with sizes ranging from 30 to 40 nm, and a strong attraction between the particles was observed. In the chitosan/Ag_2O NPs composite, the intimate connection between the nanoparticles and the polymer matrix was evident, which may explain the slight increase in particle size within the 30–40 nm range.

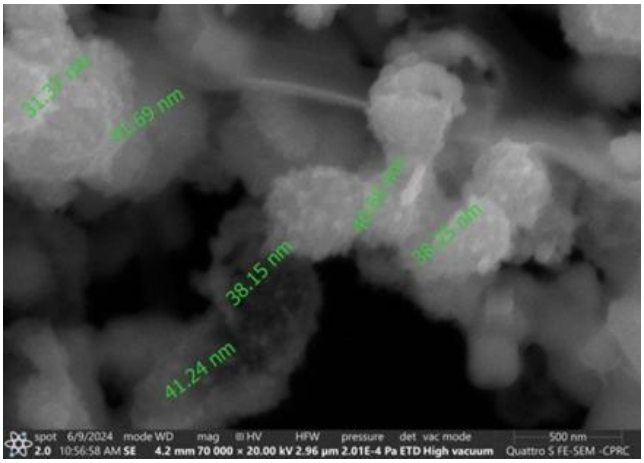

Figure (4): SEM micrograph of the synthesized Ag_2O NPs.

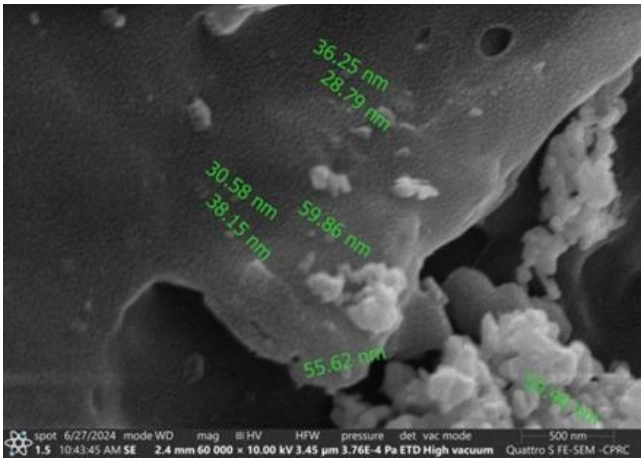

Figure (5): SEM micrograph of the synthesized chitosan/Ag_2O NPs composite.

3.1.3. X-Ray Dispersion Spectroscopy (EDS)

EDX analysis was performed to determine the elemental composition of the synthesized Ag_2O NPs and the chitosan/Ag_2O NPs composite, as shown in Figures (6 & 7) and detailed in Tables (2 & 3). Figure (6) and Table (2) confirmed the high purity of the developed Ag_2O NPs, consisting of 80.5% silver and 19.5% oxygen. In contrast, Figure (7) and Table (3) demonstrated the presence of carbon and nitrogen as the predominant elements in the composite, originating from chitosan, in addition to silver and oxygen. This provided clear evidence of the successful incorporation of chitosan into the composite matrix. Specifically, the elemental composition of the chitosan/Ag_2O NPs composite, presented in Table (3), included 45.1% carbon, 15.3% nitrogen, 39.1% oxygen, and 0.3% silver.

Table (2): The proportions of the components of synthesized Ag_2O NPs.

Element	Atomic (%)	Atomic Error (%)	Weight (%)	Weight Error (%)
O	80.5	2.6	38.0	1.2
Ag	19.5	0.0	62.0	0.1

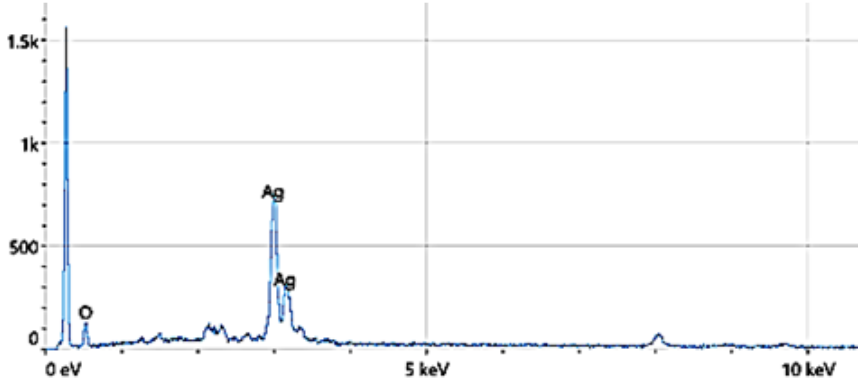

Figure (6): EDS profile of the synthesized Ag_2O NPs.

Table (3): The proportions of the components of synthesized chitosan/Ag_2O NPs composite.

Element	Atomic (%)	Atomic error (%)	Weight (%)	Weight error (%)
C	45.1	0.3	38.1	0.3
N	15.3	1.1	15.1	1.1
O	39.1	0.5	44.0	0.6
Al	0.1	0.0	0.2	0.0
Ag	0.3	0.0	2.6	0.0

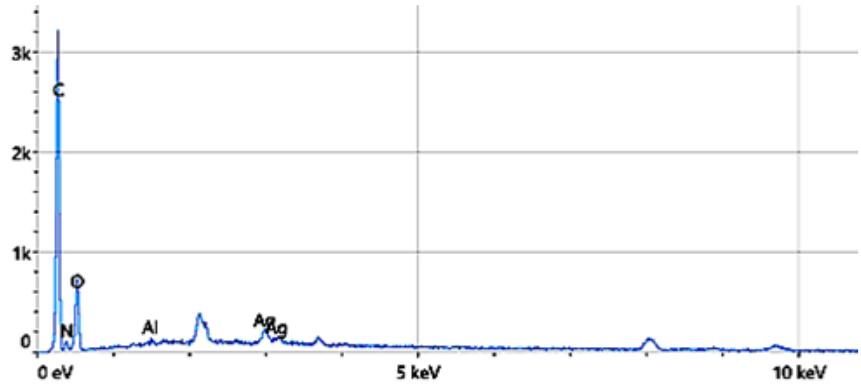

Figure (7): EDS profile of the synthesized chitosan/Ag_2O NPs composite.

3.1.4. Atomic Force Microscopy (AFM)

Figures (8 & 9) present the 2D and 3D AFM images of the Ag_2O NPs. The images revealed a rough, textured surface characterized by unevenly distributed clusters and height variations ranging from -18 nm to +22 nm. The deflection scans further confirmed the surface rigidity and strong adhesion, properties that make the material suitable for adsorption applications. Although the increased surface area enhances adsorption efficiency, some degree of agglomeration may reduce the availability of active sites, indicating potential for further optimization. Overall, the AFM analysis confirmed that the surface morphology of the Ag_2O nanoparticles is highly promising for pollutant adsorption [17, 18].

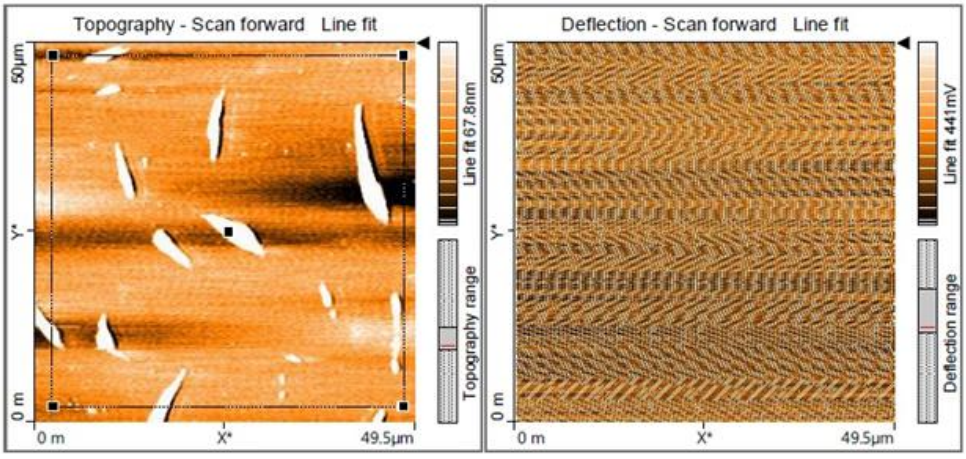

Figure (8): 2D AFM micrograph showing the surface morphology of the Ag_2O NPs film.

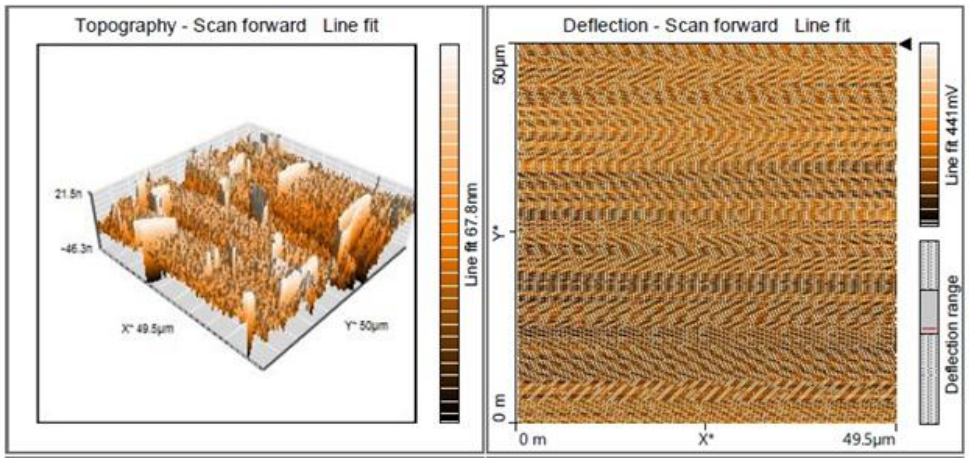

Figure (9): 3D AFM micrograph showing the surface morphology of the Ag_2O NPs film.

Figures (10 & 11) present the 2D and 3D AFM images of the chitosan/Ag_2O NPs composite. The characterization revealed a rough, heterogeneous surface morphology with height variations ranging from -82.8 nm to +150 nm. This pronounced roughness, together with high adhesion and mechanical stability, contributes to the increased surface area and enhanced adsorption capacity. The incorporation of Ag_2O NPs into the chitosan matrix results in a synergistic composite material suitable for pollutant removal. However, some degree of nanoparticle agglomeration was observed, indicating room for further optimization to maximize performance. Overall, the AFM analysis demonstrates that the composite is a promising candidate for efficient environmental remediation [19].

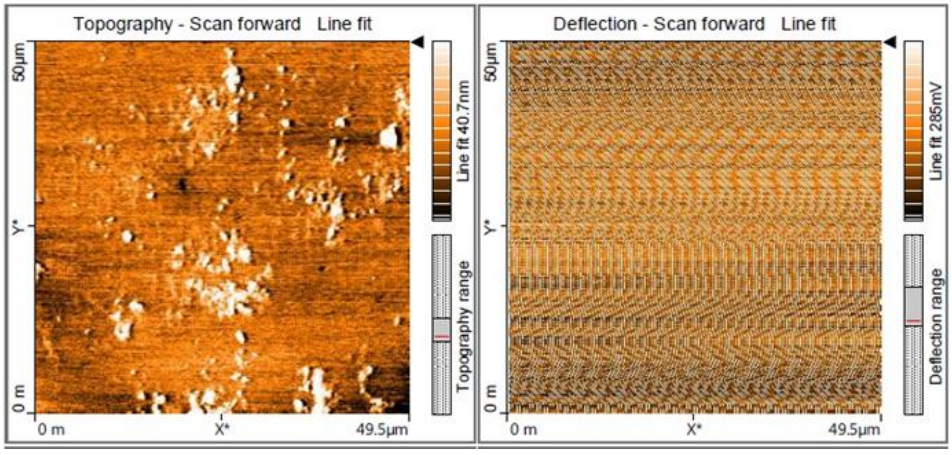

Figure (10): 2D AFM micrograph showing the surface morphology of the chitosan/Ag_2O NPs composite film.

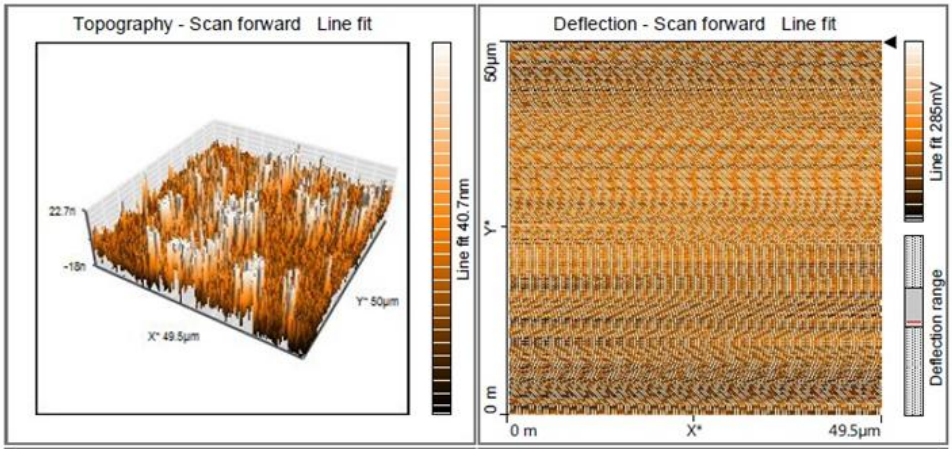

Figure (11): 3D AFM micrograph showing the surface morphology of the chitosan/Ag_2O NPs composite film.

3.1.5. X-Ray Diffraction (XRD) Analysis

XRD analysis was carried out to characterize the as-synthesized Ag_2O NPs and the chitosan/Ag_2O NPs composite, as shown in Figures (9 & 10), respectively. The XRD pattern of the Ag_2O NPs (Figure 9) exhibited six distinct diffraction peaks at 2θ values of 32.853°, 38.116°, 54.928°, 64.447°, 65.570°, and 81.473°, corresponding to the (111), (200), (202), (022), (311), and (411) crystal planes, respectively. These diffraction peaks are consistent with the ordered reference structures [20, 21], confirming the crystalline nature of the nanoparticles. The crystallite size was further calculated using the Debye–Scherrer equation (3) [22].

$$D = \frac{0.89\,\lambda}{\beta \cos\theta} \quad \text{..... (3)}$$

In the Debye–Scherrer equation, D represents the particle size, λ is the X-ray wavelength, β denotes the full width at half maximum (FWHM) of the diffraction peak in radians, and θ is the Bragg angle. The average crystallite size of the Ag_2O NPs was calculated to be approximately 25.88 nm. Figure (13) illustrates the XRD pattern of the chitosan/Ag_2O NPs composite, which retained a semi-crystalline nature. However, no well-defined diffraction peaks corresponding to Ag_2O NPs were observed, possibly due to the low doping content of the nanoparticles within the chitosan matrix.

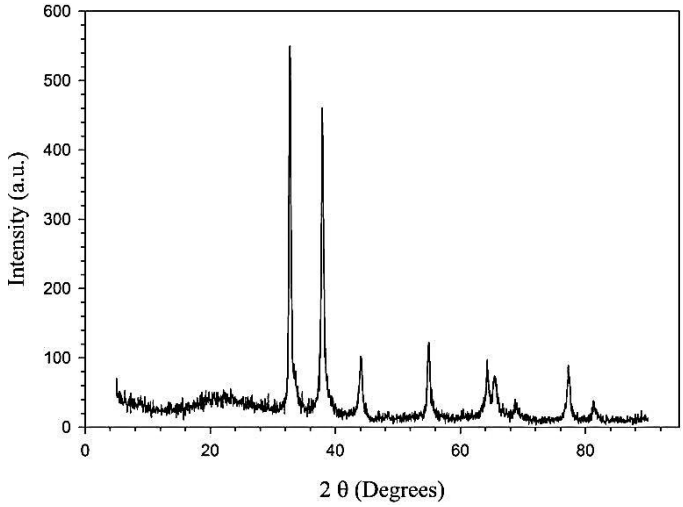

Figure (12): XRD profile of the synthesized Ag_2O NPs.

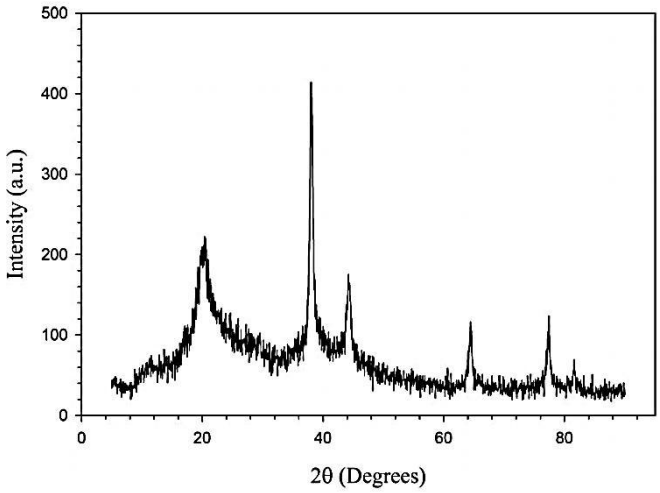

Figure (13): XRD profile of the synthesized chitosan/Ag_2O NPs composite.

3.2. The Adsorption Effect Factors

3.2.1. Effect of Adsorbent Mass

The adsorption behavior of TC at an initial concentration of 30 mg/L was investigated using chitosan/Ag_2O NPs composite at 303 K. Increasing the amount of adsorbent enhanced the available surface area and the number of active sites, thereby promoting higher TC uptake. As shown in Figure (14) and Table (4), the maximum adsorption was achieved with 0.08 g of adsorbent, indicating that the adsorption capacity had reached saturation.

Table (4): The adsorbent mass effect.

Adsorbent	m (g)	q_e (g/mg)	R (%)
chitosan/Ag_2O NPs composite	0.02	0.33956	9.055036
	0.04	1.44937	38.65005
	0.06	1.63629	43.63448
	0.08	1.92834	51.42264
	0.1	1.88161	50.17653

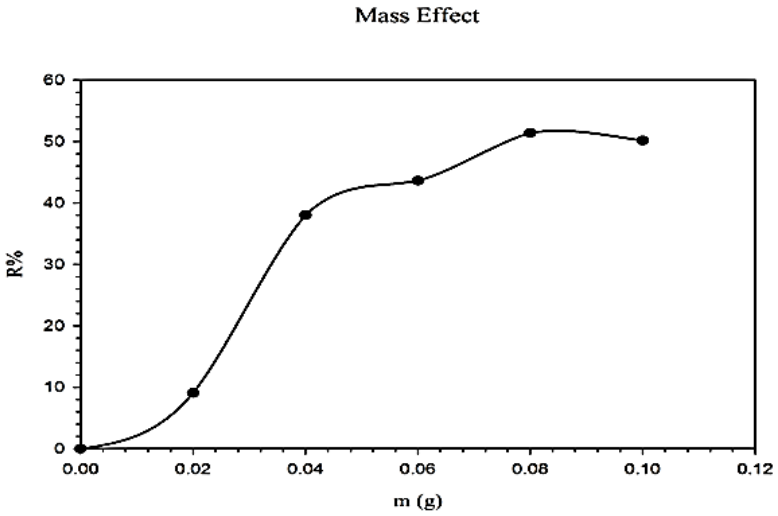

Figure (14): Quantity of TC adsorbed onto the chitosan/Ag_2O NPs composite.

3.2.2. Effect of Initial Concentration

Figure (15) and Table (5) present the adsorption profile of TC on chitosan/Ag_2O NPs composite at initial concentrations ranging from 10 to 50 mg/L, using 0.08 g of adsorbent at 303 K. The results indicate that increasing the initial drug concentration enhances adsorption, likely due to improved mass transfer and diffusion rates across the adsorbent surface. Among the tested concentrations, the highest adsorption was recorded at 30 mg/L, which was therefore selected as the optimum concentration for the study, with an equilibrium contact time of 60 min.

Table (5): Effect of varying initial TC concentration on the adsorption process.

Adsorbent	C_0 (mg/L)	q_e (mg/g)	R (%)
chitosan/Ag_2O NPs composite	10	0.608255	45.54517134
	20	1.114486	44.57943925
	30	1.792056	47.78816199
	40	1.725857	34.51713396
	50	2.446262	39.14018692

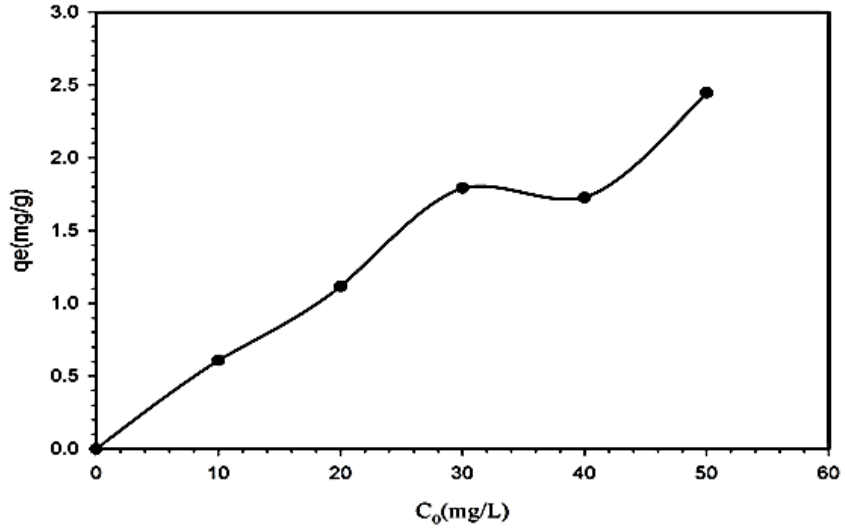

Figure (15): adsorption behavior of TC at varying initial concentration using chitosan/Ag_2O NPs composite.

3.2.3. Effect of Contact Time

The effect of contact time on the adsorption of TC onto chitosan functionalized with Ag_2O NPs was investigated at 303 K, using an initial TC concentration of 30 mg/L and 0.08 g of adsorbent in 10 mL of solution. Eight separate beakers containing identical samples were placed in a shaker under these conditions. At 15 min intervals, one beaker was removed for analysis, and this procedure continued until a total contact time of 120 min was reached. As shown in Table (6) and Figure (16), the amount of TC adsorbed increased over time and reached equilibrium after 60 min, indicating that the active sites on the adsorbent had become saturated with TC molecules, thus marking the attainment of adsorption equilibrium [23].

3.2.4. Influence of Temperature on the Removal Efficiency of TC

The removal percentage (R%) is a key indicator of adsorbent efficiency and was calculated using Equation (1) described in the Experimental Procedure section. The chitosan/Ag_2O NPs composites were tested for the adsorption of TC. The results showed that the removal efficiency was strongly influenced by temperature, with higher adsorption observed at lower temperatures, indicating the exothermic nature of the adsorption process, as presented in Table (7).

Table (6): The Contact Time Effect.

Adsorbent	t (min)	q_e (mg/g)
chitosan/Ag_2O NPs composite	0	0
	15	3.310747
	30	3.419781
	45	3.447040
	60	3.454828
	75	3.380841
	90	3.314641
	105	3.338006
	120	3.369158

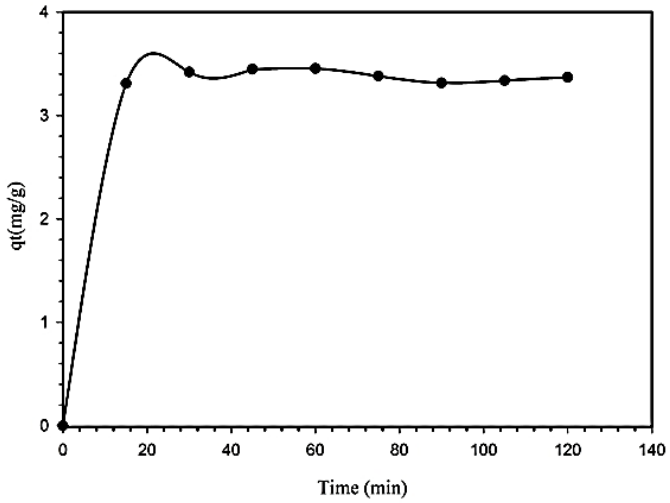

Figure (16): effect of contact time on TC adsorption by the chitosan/Ag_2O NPs composite.

Table (7): TC removal percentage onto chitosan/Ag_2O NPs surface at equilibrium under different temperatures (303, 313, and 323 K).

C_0 (mg/L)	R (%) (303K)	R (%) (313K)	R (%) (323K)
10	39.14019	37.13396	35.01558
20	44.57944	37.88162	35.23364
30	48.66044	43.36449	37.61163
40	34.51713	34.75078	31.24611
50	34.28868	33.03427	29.66978

3.3. Adsorption Isotherms

The Langmuir isotherm represents how the solute concentration in solution varies with the amount adsorbed on the adsorbent surface at constant temperature. The original (non-linear) Langmuir equation is [24]:

$$q_e = \frac{q_{max}\, K_L\, C_e}{1 + K_L\, C_e} \quad \text{..... (4)}$$

For analysis, the linear form is used:

$$\frac{C_e}{q_e} = \frac{C_e}{q_{max}} 0 + \frac{1}{q_{max}\, K_L} \quad \text{..... (5)}$$

Here, q_e refers to the amount of drug adsorbed at equilibrium (mg/g), and C_e is the drug concentration in solution at adsorption equilibrium (mg/L). The parameter q_{max} represents the maximum adsorption capacity, while K_L is the Langmuir constant obtained from experimental data. The values of q_{max} and K_L were determined from the slope and intercept, respectively, of a linear plot of C_e/q_e versus C_e. This relationship is illustrated in Figure (17).

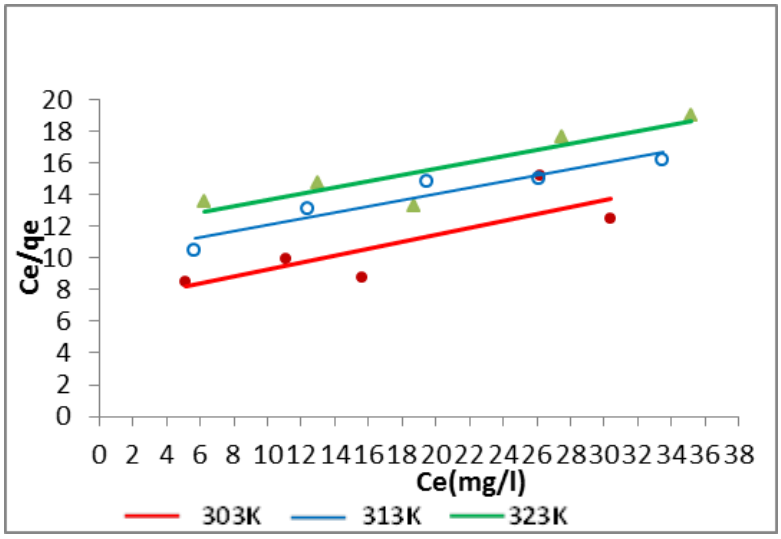

Figure (17): Temperature-dependent Langmuir isotherm plots for TC adsorbed onto the chitosan/Ag_2O NPs composite.

Table (8): Langmuir adsorption constants obtained experimentally for TC on the surface of the chitosan/Ag_2O NPs composite within the examined temperature range.

T (K)	R^2	q_{max}	K_L
303	0.67	4.5106	0.03156
313	0.8998	5.162623	0.019054
323	0.7908	5.076142	0.016906

As shown in Table (8), the values of $R^2$and K_L indicate that the adsorption system does not fit well with the Langmuir isotherm model.

The Freundlich isotherm model better represented the adsorption of TC onto the chitosan/Ag_2O NPs composite compared to the Langmuir model. The Freundlich model, as shown in Table (7), produced high values of the correlation coefficient (R^2) at all studied temperatures: 0.9228 at 303 K, 0.9977 at 313 K, and 0.9694 at 323 K. These values indicated an excellent fit and suggested a heterogeneous adsorption surface with multilayer adsorption characteristics, as shown in Figure (18). The Freundlich parameters n and K_f decreased with increasing temperature, reflecting a reduced adsorption capacity at higher temperatures, which is typical of exothermic processes.

This confirmed that the Freundlich model better explained the adsorption process of TC onto this composite, highlighting surface heterogeneity and multilayer adsorption, whereas the Langmuir model was effective but only partially [25, 26].

The Freundlich isotherm describes adsorption on heterogeneous surfaces. The original form is expressed as follows:

$$q_e = K_f C_e^{1/n} \text{ ..... (6)}$$

The linear form used for analysis is:

$$\mathbf{lnq_e = lnK_f + \frac{1}{nlnC_e}} \text{ ..... (7)}$$

Where q_e is the amount of drug adsorbed at equilibrium (mg/g), C_e is the drug concentration at equilibrium (mg/L), and K_f and n are experimental Freundlich parameters.

The values of K_f and n were obtained from the linear relationship between lnqe and lnC_e, where the intercept and slope corresponded to K_f and n, respectively, as detailed in Table (9).

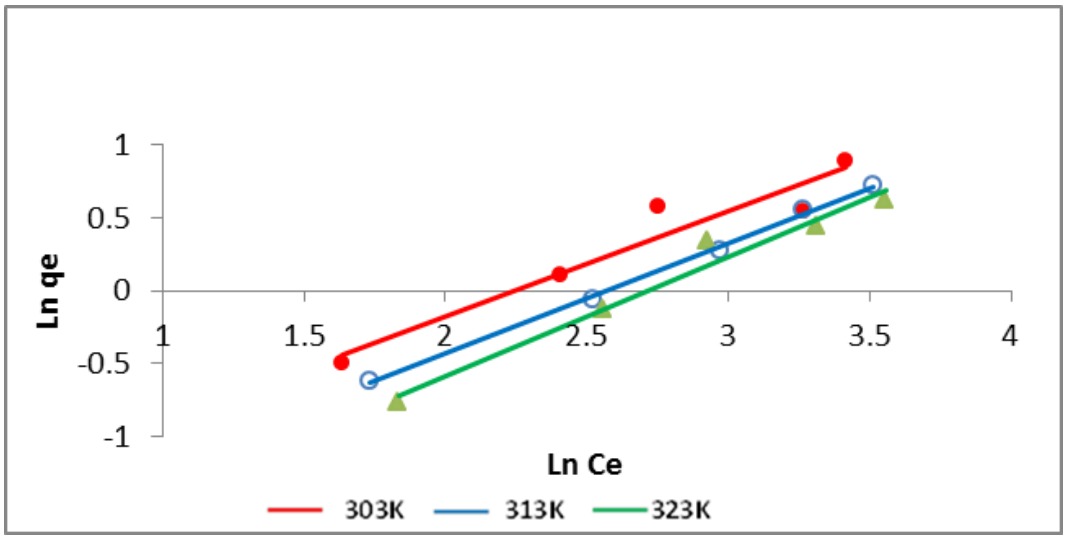

Figure (18): Freundlich isotherm curves representing the adsorption behavior of TC on chitosan/Ag_2O NPs composite across the examined temperature range.

Table (9): Freundlich isotherm constants describing TC adsorption onto chitosan/Ag_2O NPs composite at the investigated temperature conditions.

T (K)	R^2	n	K_f
303	0.9228	1.383	0.198
313	0.9977	1.321	0.174
323	0.9694	1.229	0.110

Using the linear form of the Temkin adsorption isotherm model, the adsorption of TC from solution onto the composite material chitosan/Ag_2O NPs composite was modeled at temperatures of 303, 313, and 323 K. The Temkin constants b_T and K_T were calculated from the slope and intercept, respectively, of the linear plot of q_e versus lnC_e.The Temkin model equation, as reported in [27], has been widely used to describe adsorption behavior on metal oxide nanoparticles, as illustrated in Figure (19).

$$\mathbf{q_e = b_T\, lnk_T + b_T\, lnCe} \text{ ..... (8)}$$

Where $q_e$represents the quantity of drug adsorbed at equilibrium (mg/g), b_T is an empirical constant, and C_e denotes the drug concentration remaining at equilibrium (mg/L).

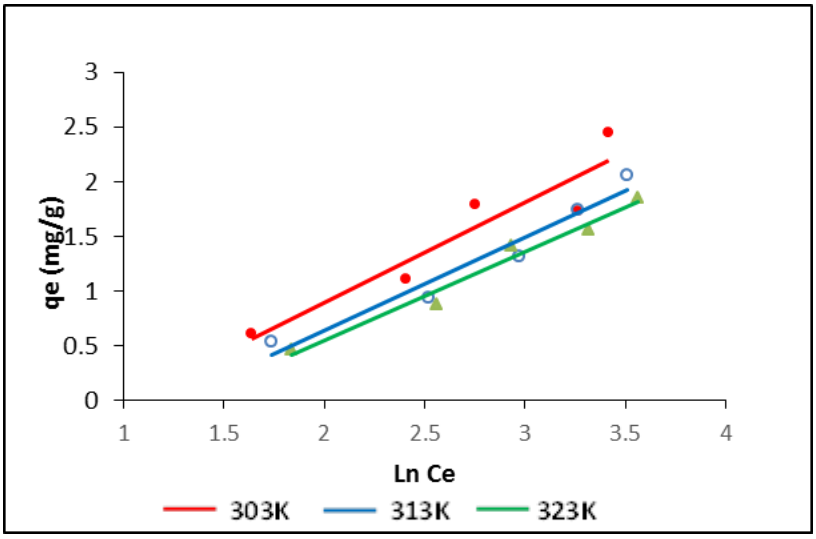

Figure (19): Linear Temkin isotherm illustrating the adsorption behavior of TC on chitosan/Ag_2O NPs composite at various temperatures.

Table (10) presents the values of the Temkin constants b_T, k_T, and the correlation coefficient R^2 calculated for the adsorption of TC onto the surface of chitosan/Ag_2O NPs composite at various temperatures. High R^2 values at all temperatures indicated that the Temkin model reliably described the adsorption behavior of this system. The decreasing K_T values with increasing temperature confirmed that the adsorption process was exothermic and less effective at higher temperatures.

Table (10): Calculated Temkin isotherm parameters describing the adsorption of TC on chitosan/Ag_2O NPs composite at different temperatures.

T (K)	(L/g)k_T	b_T	R^2
303	0.361163	0.9172	0.8774
313	0.291474	0.8432	0.9473
323	0.332365	0.9732	0.9732

3.4. Calculation Thermodynamic Functions

The effect of temperature on TC adsorption onto chitosan/Ag_2O NPs was investigated at 303, 313, and 323 K. Thermodynamic parameters, including Gibbs free energy (ΔG°), enthalpy (ΔH°), and entropy (ΔS°), were calculated to describe the adsorption process. ΔG° was obtained from the equilibrium constant (Keq) using the following equation:

$$\Delta G° = -RT \ln Kq_e \quad \ldots\ldots\ldots (9)$$

The equilibrium constants (Keq) were calculated from the Freundlich constant K_f using the Freundlich model, as expressed in Equation (6).

Here, qe is expressed in mg/g, Ce in mg/L, and n is dimensionless. Thus, Keq has units of $(L/g)^{1/n}$, ensuring consistency for adsorption and thermodynamic calculations

ΔH° was determined from the slope of lnKeq versus 1/T, while ΔS° was calculated using the following equation:

$$\Delta G° = \Delta H° - T\Delta S° \quad \ldots\ldots\ldots (10)$$

Table (11): values of the thermodynamic equilibrium constants for TC adsorption on surfaces and chitosan/Ag_2O NPs.

Adsorbent	T(K)	1/T(K^{-1})	lnK_{eq}
Chitosan/Ag_2O NPs	303	0.00330	−1.6211
	313	0.00319	−1.7491
	323	0.00309	−2.2086

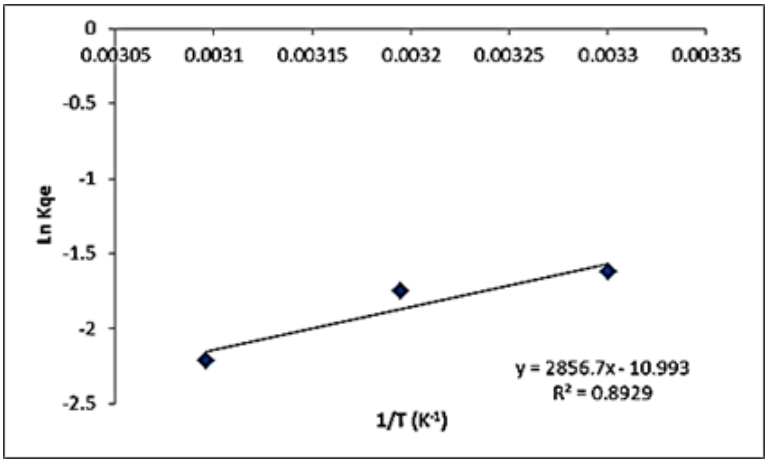

Figure (20): Vant Hoff drawings of TC adsorption on chitosan/Ag_2O NPs surface.

Table (12): The values of thermodynamic functions adsorption of TC on surfaces chitosan/Ag_2O NPs at different temperatures.

Surface	T(K)	ΔG° (kJ/mol)	slope	ΔH°(kJ/mol)	ΔS°(J/K.mol)
chitosan/Ag_2O NPs	303	+4.083781	2856.7	−23.750	−91.8607
	313	+4.551651			−90.4206
	323	+5.931023			−91.8917

Based on the data presented in Table (11), which shows the thermodynamic equilibrium constants (lnKeq) for TC adsorption onto chitosan/Ag_2O NPs at various temperatures, Van't Hoff plots were constructed and are shown in Figure (20). These plots were generated by graphing lnKeq against 1/T (K^{-1}). From the slope of the linear plots, the enthalpy change (ΔH°) of the adsorption process was calculated. This approach provided valuable insights into the thermodynamic nature of the adsorption, helping to determine whether the process was endothermic or exothermic, and to evaluate the interaction strength between TC molecules and the surface of the adsorbent.

As shown in Table (12) for chitosan/Ag_2O NPs, positive ΔG° values at all temperatures indicated that the adsorption was non-spontaneous under the studied conditions. The negative ΔH° value (–23.75 kJ/mol) confirmed the exothermic nature of the process. The large negative ΔS° values (–91.9 J/K.mol) suggested a high degree of ordering in the interactions between TC molecules and the Ag_2O NPs surface, reflecting a significant decrease in randomness. This behavior can be attributed to strong surface attraction forces and the selective affinity of TC molecules toward active sites on the adsorbent surface.

4. Conclusion

The incorporation of Ag_2O NPs into chitosan was successfully achieved, and the resulting chitosan/Ag_2O NPs composite was thoroughly characterized using FTIR, SEM, EDS, and XRD techniques. These analyses

collectively confirmed the successful synthesis, high purity, and optimal composition of the composite. Key parameters affecting adsorption, including adsorbent dosage, initial TC concentration, and contact time, were systematically investigated. The prepared composite exhibited a TC removal efficiency of approximately 51.42%, demonstrating its practical potential.

Isotherm analysis revealed that the adsorption process followed the Freundlich and Temkin models more closely than the Langmuir model. Thermodynamic evaluation indicated that TC adsorption onto chitosan/Ag_2O NPs was non-spontaneous (positive $\Delta G°$) but exothermic (negative $\Delta H°$), with highly ordered interactions between TC molecules and the Ag_2O NPs surface (large negative $\Delta S°$). These findings highlighted the crucial role of surface interactions and active sites in controlling adsorption efficiency.

For future studies, additional parameters such as pH, temperature, and coexisting ions could be investigated to enhance adsorption performance. Examining adsorption kinetics and optimizing the nanocomposite structure may further improve removal efficiency. Overall, this study demonstrated the potential of chitosan/Ag_2O NPs composite as effective adsorbents for TC removal from aqueous solutions, providing a foundation for future environmental applications.

Conflict of Interest: The authors declare that there are no conflicts of interest associated with this research project. We have no financial or personal relationships that could potentially bias our work or influence the interpretation of the results.

References

[1] W. N. Maalah and M. N. ALAzzawi, “Pollutionary effect of the Medical City wastewater on the Tigris River bacterial indicators in Baghdad city,” *Iraqi Journal of Science*, vol. 55, no. 1, pp. 106–112, 2014.
[2] F. Wang et al., “Performance of Traditional and Emerging Water-Treatment Technologies for the Removal of TC Antibiotics from Water Environments,” *Water*, vol. 14, no. 4, p. 269, 2024.
[3] A. Khezerlou et al., “MOFs-based adsorbents for the removal of TC from water,” *Scientific Reports*, vol. 15, no. 1, p. 84122, 2025.
[4] Y. Amangelsin et al., “The Impact of TC Pollution on the Aquatic Environment and Removal Strategies,” *Antibiotics*, vol. 12, no. 3, p. 440, 2023.
[5] Z. J. A. Zahra et al., “Preparation, characterization, and TC removal performance of composite adsorbents for wastewater treatment,” *Water Practice & Technology*, vol. 20, no. 4, pp. 879–890, 2025.
[6] I. Dawood, “Sustainable Water Purification through the Adsorptive Removal of TC Using Natural Clay,” *Springer Environmental Science and Pollution Research*, vol. 32, pp. 1–12, 2025.
[7] H. Kolya and C.-W. Kang, “Bio-based polymeric flocculants and adsorbents for wastewater treatment,” *Sustainability*, vol. 15, no. 12, p. 9844, 2023.
[8] E. Atangana, "Adsorption of Organic Pollutants from Wastewater Using Chitosan Derivatives," *Polymers*, vol. 17, no. 4, p. 502, 2025.
[9] M. A. Kaczorowska and D. Bożejewicz, "The Application of Chitosan-Based Adsorbents for the Removal of Hazardous Pollutants from Aqueous Solutions—A Review," *Sustainability*, vol. 16, no. 7, p. 2615, 2024.
[10] K. M. Zia, F. Jabeen, M. N. Anjum, and S. Ikram, *Biocomposites: Green Synthesis and Applications*. Elsevier, 2020.
[11] H. A. Faisal and A. K. Mohammed, "Preparation, Characterization, and TC Adsorption Efficiency of Tea Residue-Derived Activated Carbon," *Al-Khwarizmi Engineering Journal*, vol. 19, no. 4, pp. 1–15, Dec. 2023.
[12] Y. N. L. Yong, A. Ahmad, and A. W. Mohammad, “Synthesis and characterization of silver oxide nanoparticles by a novel method,” *Int. J. Sci. Eng. Res.*, vol. 3, no. 6, pp. 1–5, 2012.
[13] M. Bansal, B. Ram, G. S. Chauhan, and A. Kaushik, “L-Cysteine functionalized bagasse cellulose nanofibers for mercury (II) ions adsorption,” *International Journal of Biological Macromolecules*, vol. 112, pp. 728–736, 2018.
[14] A. J. Moahmmed and J.A.Naser et al., “Adsorption ability study of yellow (W6GS) dye from aqueous solution by Iraqi siliceous rocks,” *EM Int.*, vol. 40, no. 1, pp. 58–62, 2021.

[15] R. M. D. Ruaa, S. A. Alsahib, and I. F. Ascar, "Synthesis, characterization and cyclazation of pyran using Ag_2O nanoparticle from natural source 'GINGER'," *Iraqi Journal of Agricultural Sciences*, vol. 52, no. 5, pp. 1171–1184, 2021.
[16] S. Govindan, E. A. K. Nivethaa, R. Saravanan, V. Narayanan, and A. Stephen, "Synthesis and characterization of chitosan/silver composite," *Applied Nanoscience*, vol. 2, no. 3, pp. 299–303, 2012.
[17] Y. B. Monika et *a*l., "Surface characterization of nanoparticles using AFM," *Mater. Sci. Forum*, vol. 863, pp. 149–154, 2016.
[18] H. H. Abbas and B. A. Hasan, "The Effect of Silver Oxide on the Structural and Optical Properties of ZnO:AgO Thin Films," *Iraqi Journal of Science*, vol. 63, no. 4, pp. 1526–1539, 2022.
[19] R. Kumar and T. Subbaiah, "Role of agglomeration in nanoparticle applications: An AFM perspective," *Nanoscience Nanotechnol. Lett.*, vol. 6, no. 2, pp. 75–84, 2014.
[20] R. H. Hussian and D. K. Mahdi, "Investigation the structural influences of silver oxide addition in the bioactive phosphate glasses," *East European Journal of Physics*, vol. 3, pp. 321–328, 2023.
[21] F. H. Abdulrazzak, A. M. Abbas, and M. K. Mohammed, "Preparation and characterization of silver oxide nanoparticles (AgNPS) and evaluation the ratios of oxides," *Journal of Engineering and Applied Sciences*, vol. 14, Special Issue 5, pp. 9177–9184, 2019.
[22] U. Holzwarth and N. Gibson, "The Scherrer equation versus the 'Debye-Scherrer equation'," *Nat. Nanotechnol.*, vol. 6, no. 9, pp. 534–534, 2011.
[23] F. d. S. Silva et al., "Highly efficient adsorption of TC using chitosan-based magnetic composite," *Polymers*, vol. 14, no. 22, p. 4854, 2022.
[24] D. E. Al-Mammar and R. A. Mohammed, "Application of surfactant for enhancing the adsorption of azo dye onto Buckthorn tree wood surface," *Iraqi J. Sci.*, vol. 58, no. 4A, pp. 1780–1798, 2021.
[25] W. J. Sabbar and A. M. Abbas, "Adsorption of Janus Green by Flint Clay from Aqueous Solution at Different Temperatures," *Annals of the Romanian Society for Cell Biology*, vol. 25, no. 6, pp. 5706–5714, 2021.
[26] W. J. Fendi and J. A. Naser, "Adsorption Isotherms Study of Methylene Blue Dye on Membranes from Electrospun Nanofibers," *Oriental Journal of Chemistry*, vol. 34, no. 6, pp. 2884–2894, 2018.
[27] S. E. Hussain and J. A. Naser, "Preparation and characterization of nickel oxide nanoparticles and its adsorption optimization for parachlorophenol," *Eurasian Chem. Commun.*, vol. 4, pp. 1209–1217, 2022.